ANME-1 archaea drive methane accumulation and removal in estuarine sediments

Richard Kevorkian[a], Sean Callahan[a], Rachel Winstead[a], and Karen G. Lloyd[a,#]

[a]Department of Microbiology, University of Tennessee, Knoxville, Tennessee

Correspondence to Karen G. Lloyd, University of Tennessee, 307 Mossman, Knoxville, TN 37996, tel: 865-974-4224, fax: 865-974-4007, klloyd@utk.edu

Abstract

Uncultured members of the Methanomicrobia called ANME-1 perform the anaerobic oxidation of methane (AOM) through a process that uses much of the methanogenic pathway. It is unknown whether ANME-1 obligately perform AOM, or whether some of them can perform methanogenesis when methanogenesis is exergonic. Most marine sediments lack advective transport of methane, so AOM occurs in the sulfate methane transition zone (SMTZ) where sulfate-reducing bacteria consume hydrogen produced by fermenters, making hydrogenotrophic methanogenesis exergonic in the reverse direction. When sulfate is depleted deeper in the sediments, hydrogen accumulates making hydrogenotrophic methanogenesis exergonic, and methane accumulates in the methane zone (MZ). In White Oak River estuarine sediments, we found that ANME-1 comprised 99.5% of 16S rRNA genes from amplicons and 100% of 16S rRNA genes from metagenomes of the Methanomicrobia in the SMTZ and 99.9% and 98.3%, respectively, in the MZ. Each of the 16 ANME-1 OTUs (97% similarity) had peaks in the SMTZ that coincided with peaks of putative sulfate-reducing bacteria *Desulfatiglans sp.* and SEEP-SRB1. In the MZ, ANME-1, but no putative sulfate-reducing bacteria or cultured methanogens, increased with depth. Using publicly available data, we found that ANME-1 was the only group expressing methanogenic genes during both net AOM and net methanogenesis in an enrichment. The commonly-held belief that ANME-1 perform AOM is based on the fact that they dominate natural settings and enrichments where net AOM is measured. We found that ANME-1 also dominate natural settings and enrichment where net methanogenesis is measured, so we conclude that ANME-1 perform methane production. Alternating between AOM and methanogenesis, either in a single ANME-1 cell or between different subclades with similar 16S rRNA sequences

of ANME-1, may confer a competitive advantage, explaining the predominance of low-energy adapted ANME-1 in methanogenic sediments worldwide.

Abstract Importance: Life may operate differently at very low energy levels. Natural populations of microbes that make methane survive on some of the lowest energy yields of all life. From all available data, we infer that these microbes alternate between methane production and oxidation, depending on which process is energy-yielding in the environment. This means that much of the methane produced naturally in marine sediments occurs through an organism that is also capable of destroying it under different circumstances.

Main Text

Non-seep marine sediments are the third largest producers of methane on Earth, after rice production and wetlands (1). However, very little of this methane reaches the ocean floor because abundant uncultured archaea of the Methanomicrobia group, called ANaerobic MEthane oxidizers (ANME), catalyze the anaerobic oxidation of methane (AOM) (2, 3). However, the identities of the organisms that produce the majority of this methane are largely unknown in non-seep sediments, since cultured methanogenic groups are often difficult to find in methanogenic depths of coastal sediments (4). Some researchers have suggested that ANME can also be capable of methane production, mostly from studies showing that they are the most abundant putative methane-metabolizing organisms in methane-producing non-seep sediments (5–9).

However, sampling with a fine depth resolution as sediments switch from net methane removal to net methane production is required to determine whether ANME-1 might drive this shift. This is because the total population sizes of ANME-1 or other likely methanogens may be dynamic over spatial scales that are missed by studies examining only a few depths distributed throughout a sediment column.

Most microbes in marine sediments belong to uncultured genera to phyla (10), making it necessary to infer their physiologies in a natural setting rather than in axenic cultures. Some of these microbes drive sulfate reduction and methanogenesis, which are the key respiratory processes that directly or indirectly oxidize organic matter in anoxic marine sediments. The balance between diffusion and biological respiration drives a down-core shift from sulfate reduction to methanogenesis, with net removal of methane through AOM in the sulfate methane transition zone (SMTZ) at intermediate depths (11). Methanogens conserve energy by producing methane from hydrogen plus carbon dioxide, acetate, formate, or a range of methylated compounds. When methanogenesis is produced from hydrogen plus carbon dioxide, it is referred to as hydrogenotrophic methanogenesis (Eq. 1). In the SMTZ, sulfate reducers keep hydrogen concentrations low enough to make hydrogenotrophic methanogenesis exergonic in the reverse direction (12). This is possible because hydrogenotrophic methanogenesis, unique among many other respiratory mechanisms, can be made to be exergonic in the reverse direction by changing the relative concentrations of products and reactants. Hydrogenotrophic methanogenesis (Eq. 1) is reversible because 1) it has a stoichiometry of 4 molecules of hydrogen per methane molecule, giving hydrogen activities (activity is similar to concentration, after accounting for the ionic strength of the solution) a large amount of power over the thermodynamics and 2) hydrogen activities in marine sediments can be extremely low, down to ~10^{-9} times the standard state

activity (13). *In situ* measurements of porewater chemistry have demonstrated this reversal of ΔG between the SMTZ and the methane-containing zone when hydrogen concentrations decrease (14).

$$4H_{2(aq)} + CO_{2(aq)} \rightarrow CH_{4(aq)} + 2H_20 \qquad Eq.1$$

While some metabolic pathways such as the citric acid cycle are amphibolic (15), meaning they can occur in either the catabolic or anabolic direction, it is unknown whether a single organism can conserve energy from either hydrogenotrophic methanogenesis or AOM, depending on which direction is exergonic. Although cultured methanogens have been shown to catalyze methane oxidation, they cannot sustain the process, leading Valentine et al. to conclude that AOM does not occur through a reversal of the methanogenic metabolic pathway in most of the commonly-studied methanogenic strains in culture (16). However, it is possible that these methanogens could not sustain hydrogen production because they were adapted to very high energy yields (17) and could not survive on the paucity of energy afforded by AOM. ANME-1 archaea, on the other hand, have low energy requirements (18), making them good candidates for being reversible methanogens. ANME-1 are present and active in both AOM and methanogenic zones (8, 19–21), and they are phylogenetically related to cultured methanogens, belonging to the Methanomicrobia, a group for which all cultured strains are methanogens (22). Initial incomplete genomes from ANME-1 contained all of the genes required for methane production except for the one encoding N5, N10-methylene-tetrahydromethanopterin reductase (*mer*) (23, 24). More recently, *mer* has been found in ANME-1 genomes (20). ANME-1 has been shown to be enriched during methane production (5), and its biomass has variable stable carbon isotope values in nature, suggesting that it can use substrates other than methane to make biomass (7).

In order to infer physiology of uncultured ANME-1, we examined its population growth dynamics in fine-scale depth resolution in sediments of the White Oak River estuary and laboratory enrichments with publically available data (25). Sediments experiencing a consistent and known sedimentation rate offer an opportunity to substitute depth for time and test for the increase of a microbial population over a particular depth interval. An increase in total population size with depth implies that net growth must have occurred, although it may have been faster than the measured increase rate due to an unknown death rate. Similarly, a decrease in population size with increasing depth implies net death. Quantifying the absolute abundance of a particular microbial population in marine sediments, however, is inaccurate with current methods such as 16S rRNA gene amplicon libraries, quantitative PCR (qPCR) and Fluorescent In Situ Hybridization (FISH) (26–28). However, two of these methods, 16S rRNA gene amplicon libraries and qPCR, are quantitative in relative terms when comparing samples with similar DNA extraction and amplification biases (27, 28). Therefore, in order to measure increases or decreases in population size with depth, one can determine the change in the Fraction Read Abundance times total Cell count (FRAxC) with depth (29).

We examined 16S rRNA gene sequence FRAxC with high depth resolution (3 cm intervals in the upper 10 cm, 1 cm intervals between 10 and 60 cm, and then 3 cm intervals from 60 to 80 cm below the sediment-water interface) throughout a diagenetic sequence in sediments of the marine-influenced White Oak River estuary. Due to sediment volume restrictions from the small depth intervals, 16S rRNA gene amplicon libraries, cell counts, and hydrogen concentrations were measured for one core (core 6), sulfate concentrations were measured for the other (core 1), and methane concentrations and $\delta^{13}C$ values were measured on both cores. The fine depth resolution allowed us to visualize any die-off and regrowth of ANME-1 between

AOM and methanogenic zones, which would suggest that different ANME-1 populations perform each of the two metabolisms. The finescale approach also allowed the potential detection of cultured methanogens in any of the sediment layers that may have been missed in previous studies of estuarine sediments.

Results/Discussion

Total cell abundance decreased sharply within the first 10 cm from 2.0 x 10^8 to 2.6 x 10^7 cells/g and remained steady at ~1.3 x 10^7 cells/g for the rest of the core (Fig. 1a). Sulfate concentrations in core 1 decreased from a surficial concentration of 11.2 mM to a constant concentration of 0.06 ± 0.02 mM at 65 to78 cm (Fig. 1e). This concave decrease in sulfate is consistent with it being consumed by sulfate-reducing bacteria (30). Aqueous methane concentrations were ~0.004 mM in near-surface sediment and increased to >0.6 mM at 60 cm in core 6 (Fig. 1f) and 75 cm in core 1 (Fig. 1b), with a generally concave shape indicating AOM. Below this, methane increased to 0.73-0.87 mM in the 75-78 cm depth interval of both cores. In core 6, methane concentrations the methane concavity shifted between ~55 cm and 73 cm, consistent with methanogenesis. Between 2.5 cm and 64.5 cm, hydrogen concentrations were low (0.07 - 2.05 nM) in core 6 (Fig. 1d), consistent with those predicted for sulfate reducers operating at their minimum energy (1.22 ± 0.45 nM in similar sediments, which yields a ΔG of -20 kJ/mol sulfate, just slightly above the minimum free energy conservation (13)). Below this, hydrogen increased above 6 nM, higher than the threshold for energy conservation for hydrogenotrophic methanogenesis at 5.11 nM in similar sediments (13). In core 1, $\delta^{13}C$ of methane decreased from -41‰ ± 1.17 at 41.5 cm to -72‰ ± 0.10 at 73.5 cm (Fig 1g). In core 6,

151 $\delta^{13}C$ of methane decreased from -46‰ ± 0.20 at 29.5 cm to -74‰ ± 0.02 at 67.5 cm (Fig. 1c).
152 These values are consistent with the biogenic production of methane deeper in the sediments,
153 resulting in enrichment of the lighter carbon isotope, ^{12}C (31). Within the SMTZ, methane
154 diffusing up through the sediment became gradually depleted in the lighter carbon isotope,
155 consistent with AOM (32). This is because biological AOM has a preference for ^{12}C over ^{13}C,
156 leaving the residual methane ^{13}C-enriched (33, 34). The shift in $\delta^{13}C$-CH_4 toward "heavier"
157 values between ~60 and 30 cm indicates methane oxidation occurs in this depth interval.
158 Methane concentrations in samples shallower than the AOM zone were too low to get accurate
159 $\delta^{13}C$ values, so the values in the upper parts of the cores were not used. Together, these
160 geochemical measurements suggest the location of AOM (30 to ~60 cm) and methanogenesis
161 (>60 cm) in core 6, the core where DNA measurements were made. The depth of the onset of net
162 methanogenesis was chosen at ~60 cm because it is the depth where 1) sulfate is depleted in core
163 1, 2) hydrogen concentrations begin to continuously increase in core 6, 3) methane
164 concentrations are concave-down, and 4) $\delta^{13}C$ values become consistent with methanogenesis.
165 The upper limit of AOM is defined by the depth at which methane concentrations begin to
166 continuously increase downcore, which is 25 cm in core 6 and 45 cm in core 1. For consistency
167 in nomenclature based on the available substrates, we refer to the depths where methane is
168 present above 60cm the SMTZ, and the depths below 60cm the MZ, for methane zone.

169 ANME-1 dominated the Methanomicrobia in 16S rRNA gene amplicon libraries in both
170 the SMTZ and MZ (99.5 and 99.9%, respectively, Fig. 2). In previous work, ANME-1 were
171 shown to express methyl coenzyme M reductase subunit A (*mcrA*) genes, a key gene in
172 methanogenesis and AOM (36), in both of these zones as well (8). ANME-1 comprised six
173 OTUs of ANME-1a, nine OTUs of ANME-1b, and one ANME-1 OTU that could not be placed

into one of those two subgroups. This agrees with previous observations from Aarhus Bay (20), White Oak River estuary (8), Gulf of Mexico deep-sea (19), and Santa Barbara Basin deep-sea (21) that ANME-1 were the dominant or only organisms with the genes for methane-cycling in AOM and methanogenic sediments. Each of these analyses utilized 16S rRNA primers capable of amplifying cultured methanogens, so the absence of cultured methanogens was not likely to be an artifact of primer bias. However, primer bias can greatly skew the relative abundance of different clades (26), so we analyzed 16S rRNA gene sequences from unamplified metagenomes from the White Oak River estuary (37) and found that ANME-1 comprised 100% of the Methanomicrobia in the AOM zone and 92.86% in the MZ, in agreement with amplicon data (Fig. 2).

The four most abundant ANME-1 OTUs, comprising 96% of all ANME-1 16S rRNA gene sequences, had one or more FRAxC peaks in the SMTZ that coincided with peaks in putative sulfate-reducing bacteria *Desulfatiglans sp.* and SEEP-SRB1 (Fig. 3). SEEP-SRB1 have been shown to form syntrophies with ANME-1 (25). *Desulfatiglans sp.* have not previously been associated with syntrophies with ANME-1, but were the most abundant sulfate-reducing bacteria in ANME-1-dominated methane seeps in the Gulf of Mexico (38). In White Oak River estuary sediments, *Desulfatiglans sp.* and SEEP-SRB1 comprised 99.9% of 16S rRNA gene sequences of known sulfate-reducing bacteria clades in both the SMTZ and MZ. They were distinct from the dominant clades present in the upper, methane-free sulfate reduction zone: *Desulfobulbus sp.* and the uncultured Sva0081 clade within the Desulfobacteraceae (94% of sulfate-reducing bacteria above 25 cm, Fig. 2). The dominance patterns of these potentially sulfate-reducing clades is supported by metagenomic data as well (Fig. 2). This suggests that *Desulfatiglans sp.* and SEEP-SRB1 may be adapted to syntrophy with ANME-1 in the SMTZ, and this may allow

197 them to out-compete other sulfate-reducing bacteria deeper in the core when ANME-1 are
198 abundant.

199 The most abundant ANME-1b OTU, which accounted for 83% of total ANME-1 reads,
200 did not undergo a population decrease at the base of the SMTZ followed by an increase in the
201 MZ (Fig. 3a), as was suggested in a previous experiment with lower depth resolution (8). This
202 suggests that, for most ANME-1b, if they switch from methane-oxidizing to methane-producing,
203 this either does not require a die-off followed by a separate population growing up, or the
204 population decrease happens in a smaller depth interval than we could observe with 1 cm
205 intervals. A third possibility is that a population decrease does occur between the SMTZ and
206 MZ, but seasonal variability of SMTZ depth (8) dampens the coherence of this signal. Two
207 ANME-1b OTUs decreased with depth in the MZ (Fig. 3b and 3d). This suggests that either
208 reversibility is not universal among ANME-1 subpopulations, or that some subpopulations were
209 outcompeted by other ANME-1 in the MZ. One ANME-1a OTU, which accounted for 3% of the
210 total ANME-1 reads, did decrease at the base of the SMTZ and increase in the MZ, suggesting
211 that die-off and regrowth may be required for some ANME-1 populations to switch between
212 methane oxidation and production. In total, ANME-1 populations increased relative to those of
213 sulfate-reducing bacteria throughout the transition from SMTZ to MZ (Fig. 4).

214 The most abundant *Desulfatiglans sp.* OTU maintained its population through the MZ,
215 and all others decreased, suggesting that successively smaller populations were capable of
216 meeting their energetic needs on either cryptic sulfur cycling or fermentation as substrates were
217 depleted with depth (Fig. 4). The coupling of ANME-1 and sulfate-reducing bacteria populations
218 in the SMTZ, and their decoupling in the MZ, is consistent with ANME-1 switching from AOM,
219 which requires a sulfate-reducing partner, to methanogenesis, which does not. ANME-1a and

ANME-1b were three- and five-fold higher in the SMTZ than in the MZ. The amount of methane that is produced over many tens of centimeters of sediment depth in the MZ is consumed over just a few centimeters sediment depth in the AOM zone. Therefore, a reversible methanogen operating at similar cell specific metabolic rates in the SMTZ and MZ would be expected to be in a higher cell density in the SMTZ than in the MZ, as was observed.

The only non-ANME-1 member of the *Methanomicrobia* detected was one OTU of *Methanobacterales*, which ranged from 0 to 0.0026 % relative sequence abundance and decreased with depth in the MZ (Fig. 2), suggesting that it was not driving methanogenesis. The uncultured phylum, *Bathyarchaeota*, has been suggested to perform methane-cycling (39, 40) and increased in relative abundance with depth in the MZ (Fig. 2). However, the inference that *Bathyarchaeota* perform methane-cycling is based solely on the presence of an evolutionarily-divergent *mcrA* gene found in genomes from a terrestrial coal bed (39). Orthologs to this *mcrA* have been shown to catalyze butane rather than methane oxidation (41) and none of the *Bathyarchaeota* genomes obtained from the White Oak River estuary sediments have this gene (37). Instead *Bathyarchaeota* in marine sediments appear to perform acetogenesis and fermentation of organic substrates such as proteins and lignin (42, 43). Ten *Hadesarchaeota* OTUs increased in relative abundance in the MZ (Fig 2). This uncultured archaeal phylum has numerous carbon metabolism genes in common with *Methanomicrobia* but does not have a methanogenic enzymatic pathway. Instead *Hadesarchaeota* are hypothesized to have a heterotrophic and/or nitrogen cycling lifestyle (44). A proposed methyl-reducing methanogenic archaeal lineage, WSA2 (45), was also detected in our samples. However, the 11 OTUs were in very low relative abundance and declined below 27-30 cm (Fig. 2).

No bacteria or other archaea showed changes in relative or FRAxC abundance indicative of participation in methane cycling. OTUs from sulfide-oxidizing bacteria such as *Sulfurimonas*, *Thiotrichales*, and *Thiomicrospira* were either low in abundance, not detected, or demonstrated no significant increases in relative abundance with depth. Thirty-one OTUs of the organoheterotrophic genus *Caldithrix* and phylum *Defferibacteres* declined with depth (46). Obligate iron- and manganese-reducing bacteria either did not meet abundance thresholds or were not detected. Lokiarchaeota and Woesearchaeota both decreased in relative abundance sharply with depth. *Acidobacteria*, *Bacteroidetes*, *Latescibacteria*, *Nitrospirae*, *Deferribacteres* and *Gemmatimonadetes* all decreased with depth and accounted for less than 1% of total reads per sample. *Proteobacteria* declined steadily throughout the core from ~25% of total reads initially to ~4% by the end of the core (Fig 2). *Chloroflexi*, *Aminicenantes* and *Planctomycetes* all declined gradually throughout the core profile.

These downcore results suggest that ANME-1 performs either AOM or methanogenesis, but direct evidence for this is best obtained from experimental manipulation of an enrichment culture. Fortunately, ANME-1 enrichments have previously been shown to reverse between net AOM and net methanogenesis based on hydrogen and sulfate availability (2, 25, 34). One ANME-1 enrichment was shown to contain ANME-1 as the sole archaea, as well as SEEP-SRB1 sulfate reducers, and other bacteria (2), and demonstrated that "methane consumption was reversibly inhibited" by hydrogen additions (25). Methane concentrations increased over a period of three days when hydrogen concentrations were high (> 0.5 mM), even when sulfate was present. We calculated the rate of this methane increase and found it to be equivalent to the rate of methane decrease after hydrogen was consumed (Fig. 5). As in most AOM enrichment cultures, AOM was assumed to be driven by the dominant archaea present (ANME-1); we tested

whether ANME-1 were also the dominant archaea present when the enrichments switched to net methane production.

We performed a Blast search of *mcrA* genes from all cultured methanogens and uncultured groups containing *mcrA* against the transcriptomes from these enrichments. RNA transcriptomes provide an accounting of all the genes that are being actively transcribed to RNA at the time of sampling, representing abundance and activity. We found that only ANME-1 had hits at an e-value cutoff of $<1 \times 10^{-10}$, during both net AOM and net methanogenesis, with the exception of <0.01% hits to ANME-2, another clade of AOM-performing organisms (48) in two of the AOM-performing incubations (Fig. 5). Therefore, the only organism with the genes capable of methane metabolism in each of these incubations was ANME-1, and possibly ANME-2. Wegener et al. suggested that ANME-1 decreased in metabolic activity under conditions of net methanogenesis, since sulfate reducers prefer electrons from hydrogen than from AOM (49). In partial agreement with this interpretation, sulfate-reducing bacteria transcripts and those of dissimilatory sulfite reductase subunits A and B (*dsrAB*) increased relative to non-ANME organisms after hydrogen addition, suggesting sulfate-reducing bacteria were stimulated by the hydrogen additions (Fig. 5c). However, total ANME-1 transcripts did not decrease relative to background populations of other organisms after hydrogen addition (Fig. 5c), suggesting that ANME-1 populations were similarly abundant and active under both AOM and methanogenesis. ANME-1 *mcrA* transcripts, however, were greatly elevated under AOM conditions with low H_2 (Fig. 5). This is consistent with observations for cultured methanogens, which have been shown to up-regulate *mcrA* gene expression in response to low H_2 concentration (50, 51). Collectively, these transcript data support active methane metabolism by ANME-1, and only ANME-1, during net AOM and net methanogenesis in these enrichment experiments.

Enrichments of from Hydrate Ridge and Amon Mud Volcano show similar H_2-dependent reversibility (35). In this study, washing the ANME-1 enrichments free of sulfate was sufficient to see steady methane increases over a period of 30 days, presumably fueled by hydrogen produced by fermentation of organic matter present in the enrichments. The fact that methane started being produced in less than a day and did not increase in production rate over 30 days suggests that the methane was produced by the ANME-1 that were already there, not a growing subpopulation of a different organism, since this would have caused an exponential methane increase and a substantial lag time. Adding H_2 to the headspace increased the rate 100-fold, further supporting hydrogenotrophic methanogenesis in ANME-1. The rate of methanogenesis in these experiments was much lower than that of AOM, likely because some ANME-1 cells were washed out of the system along with the sulfate. Collectively, these studies demonstrate that the evidence for ANME-1 enrichments performing methanogenesis is as strong as the commonly-accepted evidence that ANME-1 enrichments perform AOM.

If ANME-1 cells perform AOM through a reversible interspecific hydrogen transfer to sulfate-reducing bacteria, then ANME-1 must contain hydrogenases, which are enzymes capable of metabolizing hydrogen. Although ANME-1 genomes contain homologs for the hydrogenases of cultured methanogens, they have thus far been found to lack the active site (23, 25, 49). One possible explanation is that the active subunit of a typical methanogenic hydrogenase is present in ANME-1 genomes, but has not yet been sequenced because the genomes are incomplete, in a similar situation to the *mer* gene which was discovered when more genomes became available (20). Another possibility is that ANME-1 genomes contain a novel hydrogenase active site. All known methanogenic hydrogenases are from cultures grown with extremely high hydrogen concentrations (usually 80% by volume of the headspace). Obligate hydrogenotrophic

methanogens undergo major cellular rearrangements due to hydrogen limitation, such as *Methanocaldococcus jannaschii*, which produces flagella when hydrogen is low (17) and alters its central metabolic pathway by decreasing expression of H_2-dependent methylene-tetrahydromethanoptern (H_4MPT) dehydrogenase (Hmd), and increasing expression of coenzyme F_{420}-dependent methylene-H_4MPT dehydrogenase (Mtd) (52, 53). This may be because low extracellular hydrogen concentrations create a gradient that causes hydrogen, which is membrane-permeable, to "leak" out of the cell (54), making F_{420} a more efficient electron carrier than H_2. Adaptation of ANME-1 to low hydrogen conditions may explain the abundance of enzymes utilizing F_{420} rather than hydrogen (23). ANME-1 contains Mtd, which alone is sufficient for metabolizing hydrogen (55). However, the lack of the alpha catalytic subunit suggests that ANME-1 may have a variation of Mtd with high hydrogen affinity, similar to the Hmd_{II} variant of Hmd which has a high hydrogen affinity (56). Accordingly, Beulig et al. 2018 hypothesized that one of the F_{420}-reducing hydrogenases could access electrons from hydrogen either alone or in combinations with an adjacent heterodisulfide reductase or a Nuo-like oxidoreductase complex (20).

If ANME-1 has a reversible metabolism, then all the enzymes in the pathway must be reversible. Cells often ensure that metabolic reactions that are essential to the cell, yet operate at ΔG close to zero, only flow forward by employing "irreversible" enzymes. Such enzymes, such as phosphofructokinase in glycolysis, bind their product at an allosteric site away from the active site in order to disable the enzyme activity when product builds up, in order to prevent back-flow. However, all the genes of methanogenesis have been shown to be reversible (57); possibly because they are well-poised to catalyze whichever direction is exergonic. The high degree of reversibility of the hydrogenotrophic methanogenic enzymatic pathway is shown by the fact that

hydrogenotrophic methanogens express isotopic fractionation factors highly dependent on the free energy available for the reaction (52). Therefore, ANME-1 may gain energy through AOM in the SMTZ, increasing their cell abundance relative to other methanogens. Then, when hydrogen concentrations increase after sulfate is depleted, ANME-1 have a head start on these other methanogens, and can outcompete them for meager resources.

We conclude that ANME-1 performs methanogenesis in the MZ, because it is the dominant organism with the genetic capability to do so in both geochemically-characterized White Oak River estuary sediments and well-controlled laboratory experiments. This either occurs through a metabolic reversal depending on sulfate-reducing bacterial control of hydrogen concentrations (Fig. 6), or it is caused by subclades with identical 16S rRNA sequences that drive either AOM or methanogenesis. However, it does not appear to occur through a major die-off of the majority ANME-1 population at the base of the SMTZ. Our conclusion is further supported by geochemical models (12, 13), other ANME-1 enrichments (25, 35), reversibility of the methanogenic biochemical pathway (20), and dominance of ANME-1 in common marine sediments in geographically widespread areas (8, 19, 20). Although known methanogenic clades have been cultured from marine sediments and identified by gene surveys targeting cultured clades (58), we are not aware of any study that identified cultured methanogens in methanogenic marine sediments when using universal primers, except for salt marsh tidal flats which are periodically exposed to air (59). However, many studies of deep-sea sediments lack both ANME-1 and cultured methanogens (60, 61), meaning that our results should not be extrapolated to all deep-sea locations. Marine sediments are the third largest producers of methane on Earth, after rice production and wetlands, but they are only the ninth largest methane emitters (1). If ANME-1 archaea are responsible for methanogenesis in many marine sediments, then they are

some of the dominant methane emitters on Earth, in addition their better-known function as some of Earth's most efficient methane oxidizers. The prevalence of metabolically reversible ANME-1 on Earth suggests that this level of extreme metabolic flexibility may be a more widespread feature of organisms specialized to survive in ultra-low energy environments. This could be used as a guide in the search for habitable places on Earth and extraterrestrial environments.

Acknowledgments. We thank Marc Alperin for invaluable conversations about methane over 17 years, Brett Baker for conversations about the metagenomic data, Andrew Steen, Jordan Bird, Lauren Mullen, Taylor Royalty, Katherine Sipes, Katherine Fullerton, and Joy Buongiorno for assistance retrieving the sediment samples, Michael Piehler for the use of his laboratory at the UNC Institute of Marine Sciences, Frank Löffler for use of ion and flame ionized detector chromatographs, Robert Murdoch and the University of Tennessee Knoxville Bioinformatics Resource Center for computational resources, and Christopher G. Kevorkian and Alexandra Emmons for aid in analysis. This work was funded by Alfred P. Sloan Foundation Fellowship (FG-2015-65399) and NASA Exobiology (NNX16AL59G).

Methods

Sample collection and geochemistry. Two push cores (core 1 was 78 cm deep and core 6 was 75 cm deep) were collected in May 2017 (1 m) at the White Oak River Estuary Station H (34 44.490' N, 77 07.44' W), in 1.5 m water depth. Other cores (accounting for numbers 2-5) were taken and used for other projects or thrown away because they were not long enough. Using a plunger inserted from the bottom to push the core up, sediment intervals were sectioned in 3 cm intervals from 0 to 9 cm, 1 cm intervals to 60 cm and in 3 cm intervals below that. These intervals were chosen to obtain high depth resolution in the section most likely to include

anaerobic oxidation of methane. Methane, sulfate, $\delta^{13}C$ of methane, hydrogen, and cell counts were measured as described previously (29). To measure methane, sediment was quickly sub-cored with a plastic cut-off 4 ml syringe, placed into glass serum vial containing 1 ml 0.1 M KOH, sealed with a butyl rubber stopper, and shaken to mix. Methane was determined by injecting 100 µl of gas from the headspace, after shaking the bottle vigorously for 1 min, into a gas chromatograph with a flame ionization detector (Agilent, Santa Clara, CA). Due to volume limitations when slicing into 1 cm intervals, porosity was not measured in these cores, but was used from core A in a previous core (8). To measure $\delta^{13}C$ values of methane, 4 ml of headspace from the vial used for methane measurements was removed via syringe and injected into a gas bag containing hydrocarbon free zero gas (Airgas, Radnor, PA). This was then measured on a cavity ring down spectrometer using a small sample introduction module (Picarro, Santa Clara, CA). To measure hydrogen, 2 ml of carefully sub-cored sediment was placed into a 10 ml brown glass vial being careful to disturb the sediment as little as possible, sealed with a black butyl stopper, and gassed with helium. The negative control was an empty bottle gassed with helium. After 4 days equilibration at near *in situ* temperature (21°C), 500µl of headspace gas was injected into a Peak Performer 1 Reducing Compound Photometer (Peak Laboratories, Mountain View, CA). Premixed hydrogen ppm lab bottles (Airgas) were used as standards. For cell abundance, 1 ml of sediment was placed in a 2 ml screw cap tube with 3% paraformaldehyde. To measure sulfate, a 15 ml plastic tube was filled completely with sediment and centrifuged at 5,000 xg for 5 minutes. A syringe was used to remove the supernatant below the air interface. The porewater was filtered using a 0.2 µm syringe filter into 100 µl of 10% HCl to a final volume of 1 ml. Porewater sulfate concentrations were determined by ion chromatography

401 (Dionex, Sunnyvale, CA). A 10 ml cut off syringe was filled, capped with parafilm, and frozen at
402 -80°C for later molecular analysis.

403 ***Cell quantification.*** Total cell counts were determined by direct epifluorescence microscopy
404 using SYBRGold DNA stain (Invitrogen, Carlsbad, CA). Sediments were sonicated at 20%
405 power for 40 seconds to disaggregate cells from sediments and diluted 40-fold into PBS prior to
406 filtration onto a 0.2 μm polycarbonate filter (Fisher Scientific, Waltham, MA) and mounted onto
407 a slide.

408

409 ***16S Ribosomal RNA Gene Amplicons***. DNA was extracted from frozen sediments using the Fast
410 DNA kit for Soil (MP Bio, Santa Ana, CA). The V4 region was amplified using primers 806r
411 and 515f (62), as a universal primer pair for Bacteria and Archaea. A negative sample containing
412 DNA extracted from autoclaved sediment control yielded no amplification. Library preparations
413 via Nexterra kit and sequencing using an Illumina MiSeq were performed at the Center for
414 Environmental Biotechnology at the University of Tennessee in Knoxville, producing
415 14,162,094 reads total. The CLC Genomic Workbench 10.0 (CLC Bio, a QIAGEN Company,
416 Aarhus, Denmark) was used to trim adaptors and make contigs of bidirectional sequences,
417 cluster operational taxonomic units (OTUs) at 97% similarity, and classify them with the Silva
418 reference set 132 (63). 36.4% of a total of 866,834 unique sequences were removed as chimeric,
419 resulting in a total of 9,165,958 reads in 25,116 OTUs. Approximately 5% of the remaining
420 sequences were removed for not classifying as Archaea or Bacteria. Reads were then randomly
421 subset from sample libraries to the size of the smallest library (77,609) for normalization. Only
422 OTUs with at least an average of 2 reads per sample were considered, resulting in 2,307 OTUs

423 across 59 libraries. 16S rRNA genes from metagenomes from this site (37) were obtained from
424 IMG/ER, and classified analogously to the amplicon dataset.

425 ***Data analysis of published ANME-1 enrichment experiments.*** All nine transcriptomes from
426 Wegener et al., 2015, were downloaded from the NCBI SRA as fastq files, and trimmed for
427 quality with Trimmomatic 0.33 (64). Twenty-six genes for methyl coenzyme M reductase were
428 obtained from NCBI to make a custom Blast database including representatives from all major
429 cultured methanogens, and mcrA genes from MAGs of uncultured organisms. The mcrA database
430 included the following mcrA genes: *Methanospirillum hungatei* strain JF-1 (AF313805),
431 *Methanobacterium bryantii* strain DSM 863 (AF313806), Uncultured Methanobacteriaceae methanogen
432 RS-MCR12 (AF313818), Uncultured RC1 methanogen RS-MCR15 (AF313821), *Methanoculleus*
433 *bourgensis* strain DSM 3045 (AF414036), *Methanosaeta concilii* strain DSM 3671 (AF414037),
434 *Methanocaldococcus jannaschii* strain DSM 2661 (AF414040), *Methanopyrus kandleri* strain DSM 6324
435 (AF414042), *Methanosphaera stadtmanae* strain DSM 3091 (AF414047), *Methanothermococcus*
436 *thermolithotrophicus* strain DSM 2095 (AF414048), *Methanocorpusculum labreanum* (AY260441),
437 Uncultured ANME-1Guaymas archaeon (FR682814), Uncultured ANME-1 archaeon clone F17.1_30A02
438 (AY324363), Uncultured ANME-1 archaeon clone GZfos_17_30.54 (AY324369), Uncultured ANME-2
439 archaeon clone GZfos_26_28.10 (AY324370), Uncultured ANME-2 archaeon clone GZfos_35_28.12
440 (AY324371), *Methanomassiliicoccus luminyensis* strain B10 (HQ896500), Uncultured
441 Methanomicrobiales archaeon clone H07 (AY837764), Uncultured Methanomicrobiales archaeon clone
442 B12 (AY837766), Uncultured Methanomicrobiales archaeon clone C01 (AY837767), Uncultured
443 Methanosarcinales archaeon clone C05 (AY837769), Uncultured ANME-2Guaymas archaeon clone D06
444 (AY837771), Uncultured Methanosarcinales archaeon clone B09 (AY837774), Uncultured
445 Methanococcales archaeon clone D03 (AY837775), *Methanosarcina mazeii* strain C 16 (KT387805).

The NCBI Blast tool was used to obtain hits with e-values less than 1e-10 of the transcriptomes among this *mcrA* database. Rates of methane production and consumption were calculated through WebPlotDigitizer on Extended Data Figure 4 from Wegener et al., 2015, which showed methane concentrations through time when the added hydrogen concentrations were high (> 0.5 mM) or low (< 0.1 mM).

Data archiving. 16S rRNA gene sequences can be found at the NCBI Genbank short read archive with accession number PRJNA565996.

Figures

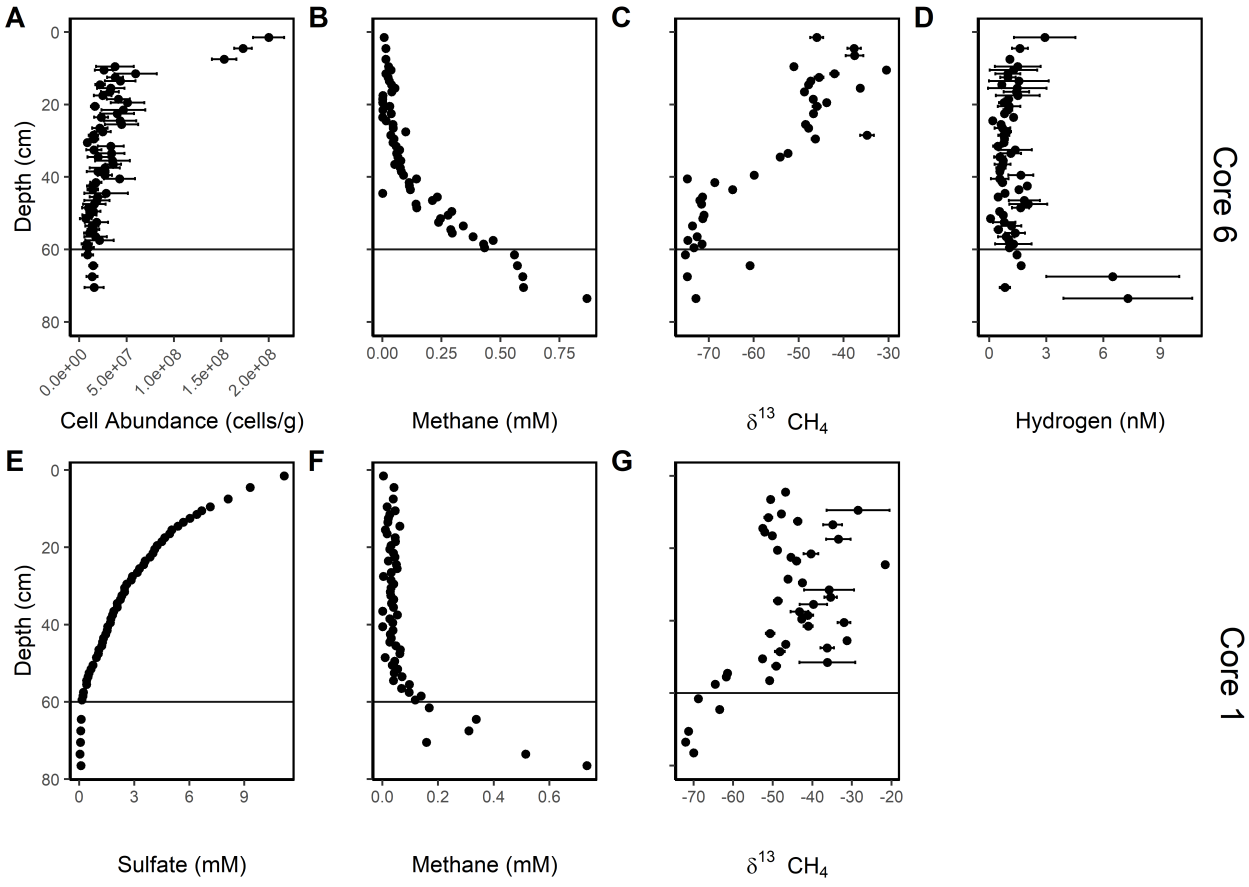

Figure 1. **White Oak River estuary cores show methane-consuming or AOM sediments in the SMTZ and methane-producing or methanogenic sediments below it.** Aqueous geochemistry for cores 6 (top row) and 1 (bottom row), with A) cell abundance, B and F) methane concentration, C and G) $\delta^{13}C$ of methane, D) hydrogen concentration, and E) sulfate concentration. Black line shows approximate transition from AOM to methanogenesis.

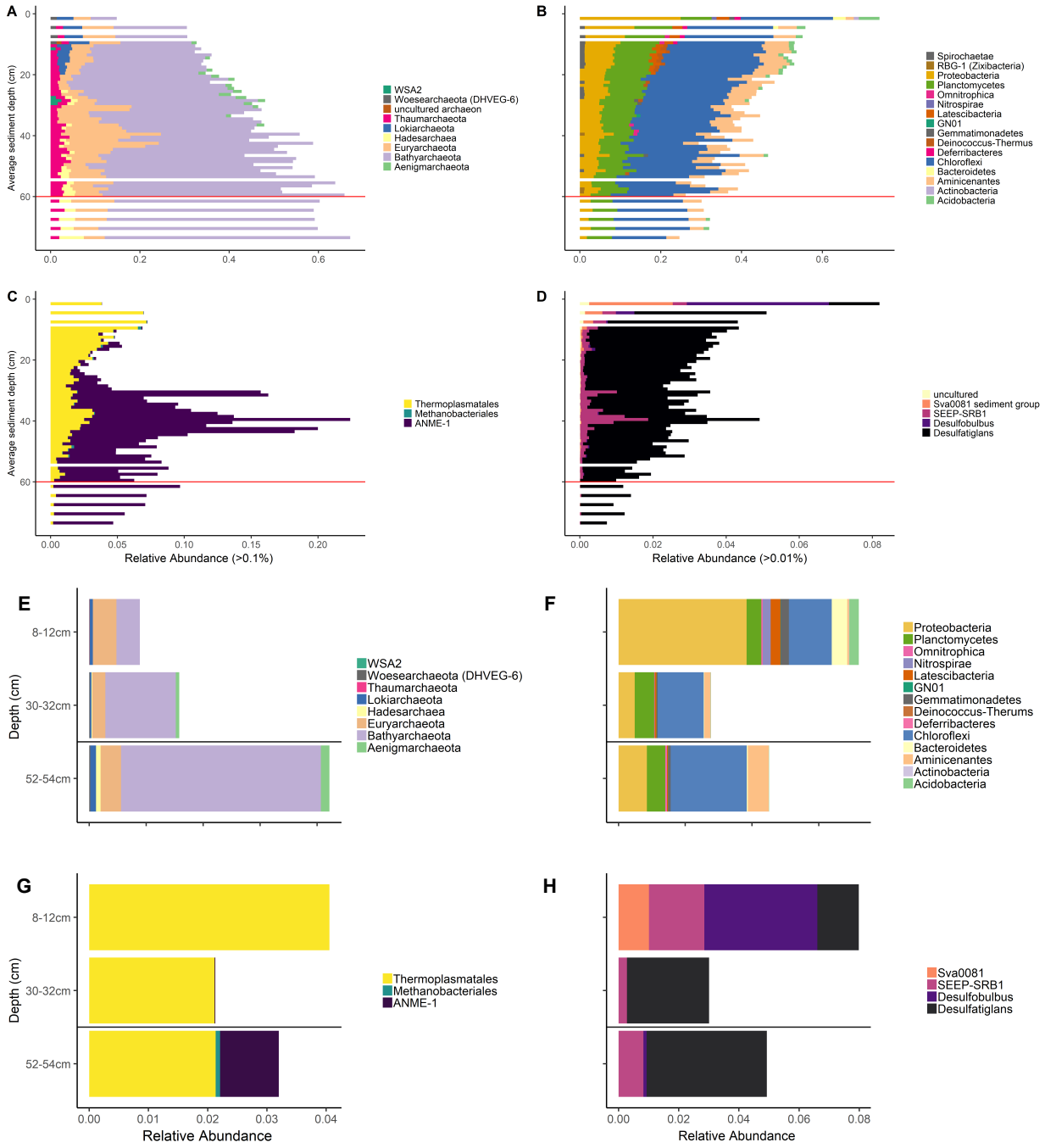

Figure 2. ANME-1 and *Desulfatiglans sp.* dominate methane- and sulfur-cycling organisms in both methane-consuming and methane-producing sediments. Relative abundance of 16S rRNA gene sequences for all archaea (left panels) and all bacteria (right panels), for amplicon libraries (A-D) and metagenomes (E-H), grouped at the phylum level. C, D, G, and H show putative sulfate-reducing bacteria and Euryarchaeota, grouped at the family level. Only phyla with >1% relative 16S rRNA gene sequence abundance for bacteria and > 0.1% for archaea are shown. Black lines show transition from AOM to methanogenesis.

454

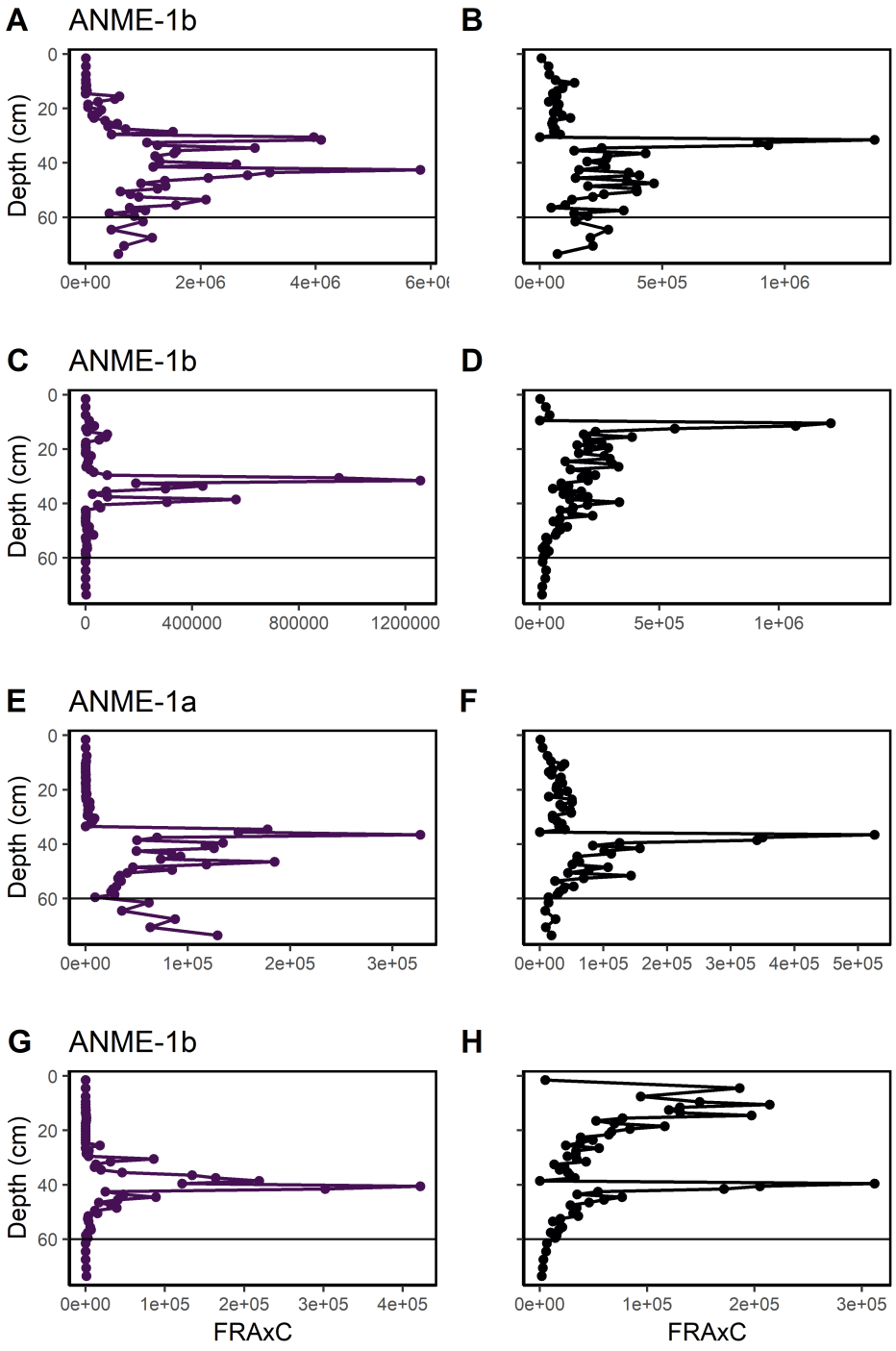

Figure 3. ANME-1 Fraction Read Abundance times Cell counts (FRAxC) and sulfate reducing bacteria have co-occurring peaks during AOM but not methanogenesis. Values for the four most abundant OTUs of ANME-1 (left panels, A, C, E, and G) and *Desulfatiglans sp.* (right panels, B, D, F, and H) with depth, ordered by decreasing OTU abundance from top to bottom panels. Colors match those in Figure 2, and black line indicates AOM to methanogenesis transition.

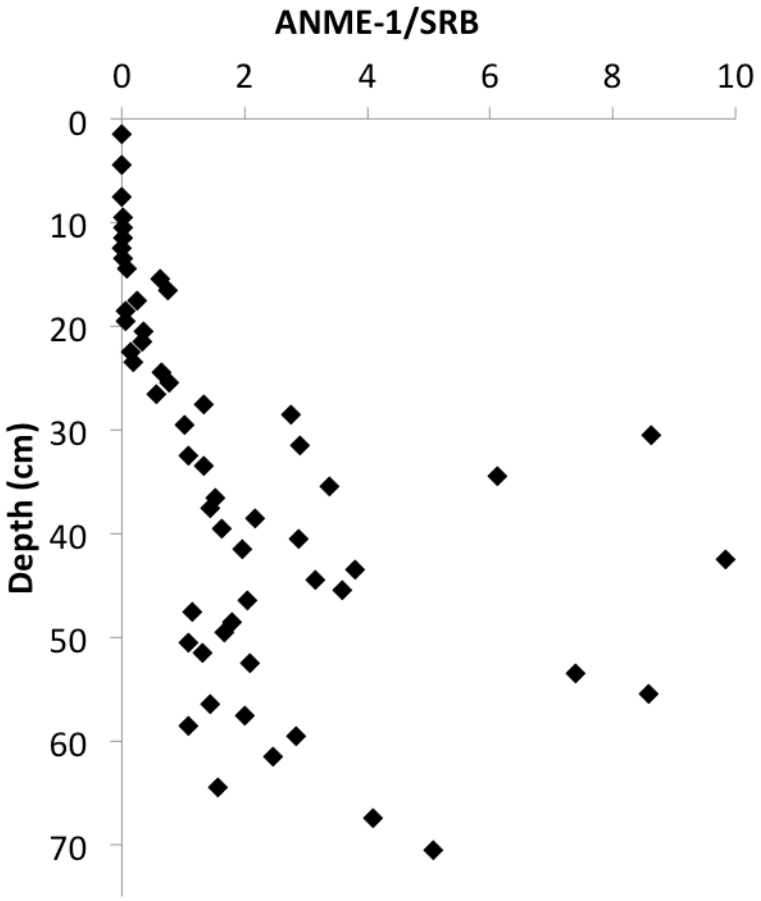

Figure 4. ANME-1 increased relative to sulfate reducing bacteria throughout the SMTZ and below. Ratio of total ANME-1 16S rRNA gene abundance to total sulfate reducing bacteria 16S rRNA gene abundance with depth.

472

473

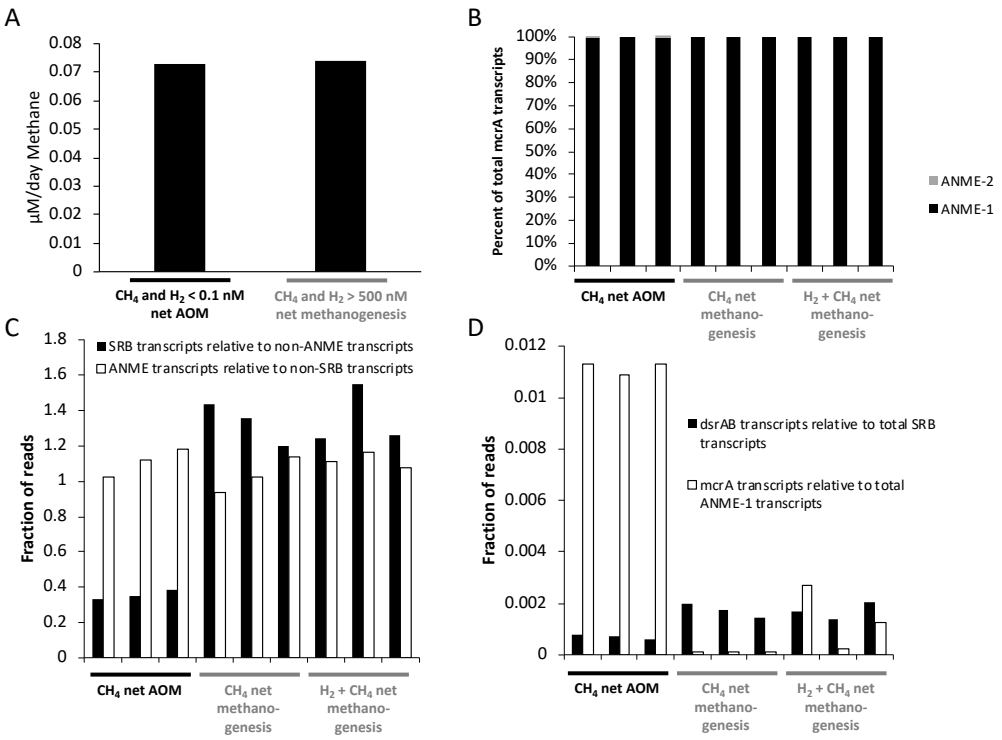

Figure 5. In laboratory enrichments, ANME-1 were likely responsible for AOM in methane-consuming conditions and methanogenesis in methane-producing conditions, controlled by the hydrogen concentration. Shown are A) rates of methane consumption or production, dependent on hydrogen concentrations, B-D) transcript read abundances when triplicates were gassed with methane alone (AOM), hydrogen alone (methanogenic), or hydrogen plus methane (methanogenic), with B) taxonomic identities of all methyl coenzyme-M reductase subunit A (*mcrA)* gene transcripts, C) relative 16S rRNA gene transcript abundance of putative sulfate reducers relative to all transcripts besides those of ANME-1 and of ANME-1 relative to all transcripts besides those of sulfate reducers, and D) transcripts of dissimilatory sulfite reductase subunits A and B (*dsrAB*) relative to total transcripts from sulfate reducing bacteria and transcripts of *mcrA* relative to total transcripts from ANME-1. Data were from A) Wegener et al., 2015 Figure S4, B) our Blast analysis of transcripts obtained from the NCBI short read archive from Wegener et al., 2015, and C and D) Wegener et al., 2015.

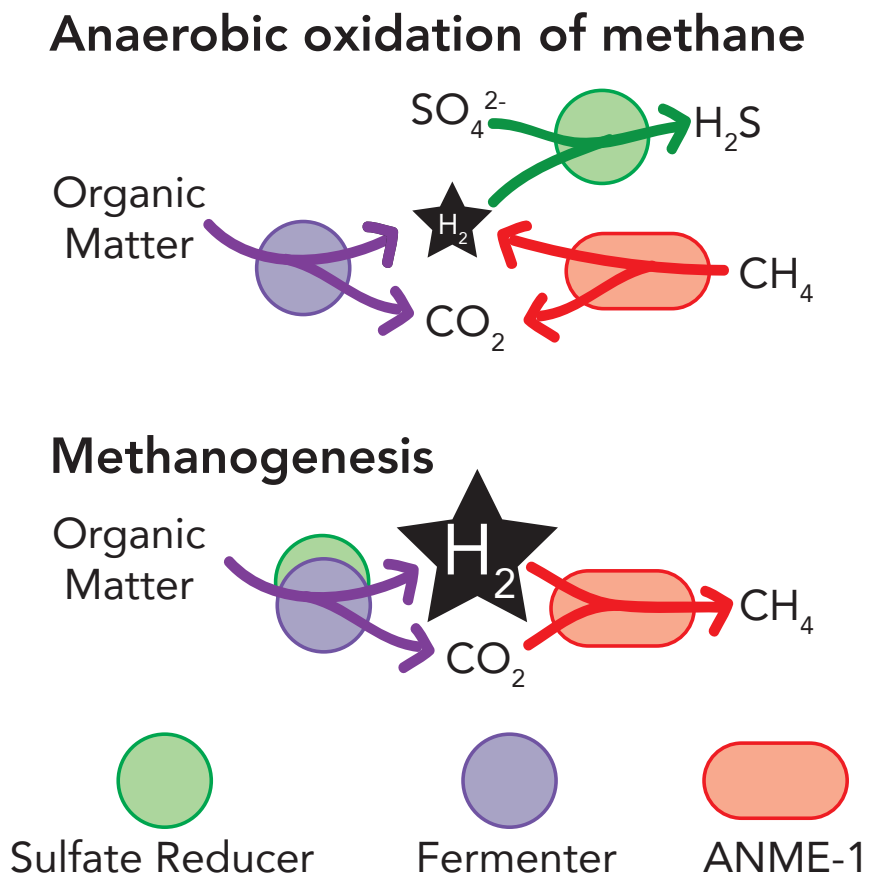

Figure 6. Model for AOM and methanogenesis in non-seep marine sediments. Fermenters produce hydrogen from organic matter under both conditions. During anaerobic oxidation of methane, sulfate reducers bring hydrogen concentrations so low that methane oxidation is exergonic. During methanogenesis, sulfate reducers have run out of sulfate so hydrogen concentrations build up to a level that makes ANME-1 switch to forward methanogenesis. Sulfate reducers may persist by switching to fermentation. Purple = fermenters, green = sulfate reducers, and red = ANME-1.

References

1. Reeburgh WS (2007) Oceanic Methane Biogeochemistry. *Chem Rev* 107:486–513.

2. Holler T, et al. (2011) Thermophilic anaerobic oxidation of methane by marine microbial consortia. *ISME J* 5(12):1946–56.

3. Knittel K, Boetius A (2009) Anaerobic oxidation of methane: Progress with an unknown process. *Annu Rev Microbiol* 63:311–334.

4. Kendall MM, et al. (2007) Diversity of Archaea in marine sediments from Skan Bay, Alaska, including cultivated methanogens, and description of Methanogenium boonei sp. nov. *Appl Environ Microbiol* 73(2):407–14.

5. Jagersma CG, et al. (2012) Enrichment of ANME-1 from Eckernförde Bay sediment on thiosulfate, methane and short-chain fatty acids. *J Biotechnol* 157(4):482–9.

6. Orcutt B, Boetius A, Elvert M, Samarkin V, Joye SB (2005) Molecular biogeochemistry of sulfate reduction, methanogenesis and the anaerobic oxidation of methane at Gulf of Mexico cold seeps. *Geochim Cosmochim Acta* 17:4267–4281.

7. House CH, et al. (2009) Extensive carbon isotopic heterogeneity among methane seep microbiota. *Environ Microbiol* 11(9):2207–15.

8. Lloyd KG, Alperin MJ, Teske A (2011) Environmental evidence for net methane production and oxidation in putative ANaerobic MEthanotrophic (ANME) archaea. *Environ Microbiol* 13(9):2548–2564.

9. Bertram S, et al. (2013) Methanogenic capabilities of ANME-archaea deduced from 13C-

labelling approaches. *Environ Microbiol* 15(8):2384–2393.

10. Lloyd KG, Steen AD, Ladau J, Yin J, Crosby L (2018) Phylogenetically novel uncultured microbial cells dominate Earth microbiomes. *mSystems* 3:e00055-18.

11. Martens S, Berner RA (1977) Interstitial water chemistry of anoxic Long Island Sound sediments. 1. Dissolved gases. *Limnol Oceanogr* 22(January):10–25.

12. Hoehler TM, Alperin MJ, Albert DB, Martens CS (1994) Field and laboratory studies of methane oxidation in an anoxic marine sediment: Evidence for a methanogen-sulfate reducer consortium. *Global Biogeochem Cycles* 8(4):451–463.

13. Hoehler TM, Alperin MJ, Albert DB, Martens CS (1998) Thermodynamic control on hydrogen concentrations in anoxic sediments. *Geochim Cosmochim Acta* 62(10):1745–1756.

14. Hoehler TM, Alperin MJ, Albert DB, Martens CS (2001) Apparent minimum free energy requirements for methanogenic Archaea and sulfate-reducing bacteria in an anoxic marine sediment. *FEMS Microbiol Ecol* 38:33–41.

15. Slonczewski JL, Foster JW (2017) *Microbiology: An Evolving Science, 4rd Ed.* (W. W. Norton & Co.).

16. Valentine DL, Blanton DC, Reeburgh WS (2000) Hydrogen production by methanogens under low-hydrogen conditions. *Arch Microbiol*:415–421.

17. Mukhopadhyay B, Johnson EF, Wolfe RS (2000) A novel pH2 control on the expression of flagella in the hyperthermophilic strictly hydrogenotrophic methanarchaeaon Methanococcus jannaschii. *Proc Natl Acad Sci U S A* 97(21):11522–7.

549 18. Nauhaus K, Albrecht M, Elvert M, Boetius A, Widdel F (2007) In vitro cell growth of
550 marine archaeal-bacterial consortia during anaerobic oxidation of methane with sulfate.
551 *Environ Microbiol* 9:187–196.

552 19. Underwood S, Lapham L, Teske A, Lloyd KG (2016) Microbial community structure and
553 methane-cycling activity of subsurface sediments at Mississippi Canyon 118 before the
554 Deepwater Horizon disaster. *Deep Res Part II* 129:148–156.

555 20. Beulig F, Røy H, McGlynn SE, Jørgensen BB (2019) Cryptic CH4 cycling in the sulfate–
556 methane transition of marine sediments apparently mediated by ANME-1 archaea. *ISME J*
557 13(2):250–262.

558 21. Harrison BK, Zhang H, Berelson W, Orphan VJ (2009) Variations in archaeal and
559 bacterial diversity associated with the sulfate-methane transition zone in continental
560 margin sediments (Santa Barbara Basin, California). *Appl Environ Microbiol* 75(6):1487–
561 99.

562 22. Whitman WB ed. (2015) *Bergey's Manual of Systematics of Archaea and Bacteria* (John
563 Wiley & Sons).

564 23. Meyerdierks A, et al. (2010) Metagenome and mRNA expression analyses of anaerobic
565 methanotrophic archaea of the ANME-1 group. *Environ Microbiol* 12:422–439.

566 24. Hallam SJ, et al. (2004) Reverse methanogenesis: testing the hypothesis with
567 environmental genomics. *Science* 305(5689):1457–62.

568 25. Wegener G, Krukenberg V, Riedel D, Tegetmeyer HE, Boetius A (2015) Intercellular
569 wiring enables electron transfer between methanotrophic archaea and bacteria. *Nature*

526:587–590.

26. Polz MF, Cavanaugh CM (1998) Bias in template-to-product ratios in multitemplate PCR. *Appl Environ Microbiol* 64(10):3724–3730.

27. Lloyd KG, May MK, Kevorkian RT, Steen AD (2013) Meta-analysis of quantification methods shows that archaea and bacteria have similar abundances in the subseafloor. *Appl Environ Microbiol* 79(24):7790–7799.

28. Buongiorno J, et al. Inter-laboratory quantification of Bacteria and Archaea in deeply buried sediments of the Baltic Sea (IODP Exp. 347). *FEMS Microbiol Ecol*.

29. Kevorkian R, Bird JT, Shumaker A, Lloyd KG (2018) Estimating population turnover rates by relative quantification methods reveals microbial dynamics in marine sediment. *Appl Environ Microbiol* 84(1):1–16.

30. Martens CS, Albert DB, Alperin MJ (1998) Biogeochemical processes controlling methane in gassy coastal sediments - Part 1. A model coupling organic matter flux to gas production, oxidation and transport. *Cont Shelf Res* 18:1741–1770.

31. Whiticar MJ (1999) Carbon and hydrogen isotope systematics of bacterial formation and oxidation of methane. *Chem Geol* 161:291–314.

32. Jørgensen BB, Kasten S (2006) *Sulfur cycling and methane oxidation* eds Schulz H, Zabel M (Springer, Berlin; Heidelberg) doi:10.1007/3-540-32144-6.

33. Alperin MJ, Reeburgh WS, Whiticar MJ (1988) Carbon and hydrogen isotope fractionation resulting from anaerobic methane oxidation. *Global Biogeochem Cycles* 2(3):279–288.

591 34. Holler T, et al. (2009) Substantial 13C/12 C and D/H fractionation during anaerobic
592 oxidation of methane by marine consortia enriched in vitro. *Environ Microbiol Rep*
593 1(5):370–376.

594 35. Yoshinaga MY, et al. (2014) Carbon isotope equilibration during sulphate-limited
595 anaerobic oxidation of methane. *Nat Geosci* 7:190–194.

596 36. Shima S, et al. (2012) Structure of a methyl-coenzyme M reductase from Black Sea mats
597 that oxidize methane anaerobically. *Nature* 481(7379):98–101.

598 37. Lazar CS, et al. (2016) Genomic evidence for distinct carbon substrate preferences and
599 ecological niches of Bathyarchaeota in estuarine sediments. *Environ Microbiol*
600 18(4):1200–1211.

601 38. Lloyd KG, Lapham L, Teske A (2006) An anaerobic methane-oxidizing community of
602 ANME-1b archaea in hypersaline gulf of Mexico sediments. *Appl Environ Microbiol*
603 72(11). doi:10.1128/AEM.00886-06.

604 39. Evans PN, et al. (2015) Methane metabolism in the archaeal phylum Bathyarchaeota
605 revealed by genome-centric metagenomics. *Science (80-)* 350(6259):434–8.

606 40. Kubo K, et al. (2012) Archaea of the Miscellaneous Crenarchaeotal Group are abundant,
607 diverse and widespread in marine sediments. *ISME J* 6(10):1949–1965.

608 41. Laso-Peréz R, Wegener G, Knittel K, Widdel F (2016) Thermophilic archaea activate
609 butane via alkyl-CoM formation. *Nature*:1–36.

610 42. He Y, et al. (2016) Genomic and enzymatic evidence for acetogenesis among multiple
611 lineages of the archaeal phylum Bathyarchaeota widespread in marine sediments. *Nat*

612 *Microbiol* 35:1–9.

613 43. Lloyd KG, et al. (2013) Predominant arcahea in marine sedimetns degrade detrital
614 proteins. *Nature*:1–6.

615 44. Baker BJ, et al. (2016) Genomic inference of the metabolism of cosmopolitan subsurface
616 Archaea, Hadesarchaea. *Nat Microbiol* 1(3):1–7.

617 45. Nobu MK, Narihiro T, Kuroda K, Mei R, Liu WT (2016) Chasing the elusive
618 Euryarchaeota class WSA2: Genomes reveal a uniquely fastidious methyl-reducing
619 methanogen. *ISME J* 10(10):2478–2487.

620 46. Miroshnichenko ML, Kolganova T V., Spring S, Chernyh N, Bonch-Osmolovskaya EA
621 (2010) Caldithrix palaeochoryensis sp. nov., a thermophilic, anaerobic, chemo-
622 organotrophic bacterium from a geothermally heated sediment, and emended description
623 of the genus Caldithrix. *Int J Syst Evol Microbiol* 60(9):2120–2123.

624 47. Nauhaus K, Treude T, Boetius A, Krüger M (2005) Environmental regulation of the
625 anaerobic oxidation of methane: A comparison of ANME-I and ANME-II communities.
626 *Environ Microbiol* 7(1):98–106.

627 48. Orphan VJ, House CH, Hinrichs K, Mckeegan KD, Delong EF (2001) Methane-
628 consuming archaea revealed by directly coupled isotopic and phylogenetic analysis.
629 *Science (80-)* 293(5529):484–487.

630 49. Krukenberg V, et al. (2018) Gene expression and ultrastructure of meso- and thermophilic
631 methanotrophic consortia. *Environ Microbiol* 20(5):1651–1666.

632 50. Nölling J, Reeve JN (1997) Growth- and substrate-dependent transcription of the formate

633 dehydrogenase (fdhCAB) operon in Methanobacterium thermoformicicum Z-245. *J*
634 *Bacteriol* 179(3):899–908.

635 51. Kato S, Kosaka T, Watanabe K (2008) Comparative transcriptome analysis of responses
636 of Methanothermobacter thermautotrophicus to different environmental stimuli. *Environ*
637 *Microbiol* 10(4):893–905.

638 52. Topçuoglu BD, Meydan C, Nguyen TB, Lang SQ, Holden JF (2019) Growth kinetics,
639 carbon isotope fractionation, and gene expression in the hyperthermophile
640 Methanocaldococcus jannaschii during hydrogn-limited growth and interspecies hydrogen
641 transfer. *Appl Environ Microbiol* 85(9):1–14.

642 53. Hendrickson EL, Haydock AK, Moore BC, Whitman WB, Leigh JA (2007) Functionally
643 distinct genes regulated by hydrogen limitation and growth rate in methanogenic Archaea.
644 *Proc Natl Acad Sci USA* 104:8930–8934.

645 54. Finke N, Hoehler TM, Jørgensen BB (2007) Hydrogen "leakage" during methanogenesis
646 from methanol and methylamine: implications for anaerobic carbon degradation pathways
647 in aquatic sediments. *Environ Microbiol* 9(4):1060–71.

648 55. Hendrickson EL, Leigh JA (2008) Roles of coenzyme F420-reducing hydrogenases and
649 hydrogen- and F420-dependent methylenetetrahydromethanopterin dehydrogenases in
650 reduction of F420 and production of hydrogen during methanogenesis. *J Bacteriol*
651 190(14):4818–4821.

652 56. Walker CB, et al. (2012) Functional responses of methanogenic archaea to syntrophic
653 growth. *ISME J* 6(11):2045–2055.

654 57. Scheller S, Goenrich M, Boecher R, Thauer RK, Jaun B (2010) The key nickel enzyme of
655 methanogenesis catalyses the anaerobic oxidation of methane. *Nature* 465(7298):606–608.

656 58. Lever MA (2013) Functional gene surveys from ocean drilling expeditions - a review and
657 perspective. *FEMS Microbiol Ecol* 84:1–23.

658 59. Wilms R, Sass H, Ko B, Cypionka H, Engelen B (2006) Specific bacterial, archaeal, and
659 eukaryotic communities in tidal-flat sediments along a vertical profile of several meters.
660 *Appl Environ Microbiol* 72(4):2756–2764.

661 60. Vetriani C, Jannasch HW, Gregor BJMAC, Stahl DA, Reysenbach A (1999) Population
662 structure and phylogenetic characterization of marine benthic archaea in deep-sea
663 sediments. *Appl Environ Microbiol* 65(10):4375–4384.

664 61. Biddle JF, et al. (2006) Heterotrophic archaea dominate sedimentary subsurface
665 ecosystems off Peru. *Proc Natl Acad Sci USA* 103(10):3846–3851.

666 62. Caporaso JG, et al. (2012) Ultra-high-throughput microbial community analysis on the
667 Illumina HiSeq and MiSeq platforms. *ISME J* 6:1621–1624.

668 63. Pruesse E, et al. (2007) SILVA: a comprehensive online resource for quality checked and
669 aligned ribosomal RNA sequence data compatible with ARB. *Nucleic Acids Res*
670 35(21):7188–7196.

671 64. Bolger AM, Lohse M, Usadel B (2014) Trimmomatic: a flexible trimmer for Illumina
672 sequence data. *Bioinformatics* 30(15):2114–2120.

673